行政院國家科學委員會專題研究計畫 成果報告

光纖光放大器與波長轉換器四波混合效應研究
研究成果報告(精簡版)

計 畫 類 別 ：個別型
計 畫 編 號 ：NSC 95-2221-E-216-044-
執 行 期 間 ：95 年 08 月 01 日至 96 年 07 月 31 日
執 行 單 位 ：中華大學電機工程研究所

計 畫 主 持 人：溫盛發

計畫參與人員：碩士班研究生-兼任助理：張燕華、歐峻瑋

處 理 方 式 ：本計畫可公開查詢

中 華 民 國 96 年 10 月 30 日

行政院國家科學委員會專題研究計畫成果報告

光纖光放大器與波長轉換器四波混合效應研究

Studies of four-wave mixing effects in optical fiber amplifiers and wavelength converters

計畫編號：NSC 95-2221-E-216-044
執行期限：95 年 8 月 1 日至 96 年 7 月 31 日
主持人: 溫盛發　　中華大學 電機系

一、中文摘要

原計畫書推導電場頻率分量之耦合聯立方程式，以描述在光放大器與光波長轉換器中前向與反向光波之非線性交互作用，例如包括四波混合，拉曼效應，與布里安效應。所提出的方法可以完整描述前向與反向行進光波的頻率域與時域之行為，突破緩變包絡近似之限制。但要付出很耗數值模擬時間的代價，因此需要使用電腦叢集做平行運算，使計算時間在可以接受的範圍內。由於核定之儀器設備費幾乎全部遭刪除，很難進行數值模擬計算。因此本計畫改為進行基於光功率耦合方程式之研究，使數值模擬計算時間可以接受，但已更改原計畫之目標。儘管如此，更改後之計畫研究成果已刊登於 Optics Express 與 Optics Communications 各一篇，以及投稿 Journal of Optical Society of America B 一篇。已刊登之論文內容請參考期刊論文全文，本報告只說明已投稿但尚未刊登之論文內容。

本論文提出一個擾動方法分析信號光，幫浦光，與亞穩態鉺離子密度之間的交互作用，以研究在摻鉺光纖放大器中之快速光。探討幫浦光時域變化對快速光的影響，其中幫浦光時域變化是幫浦光功率對亞穩態粒子密度時域變化的響應。由於做了微小信號光功率的假設，這個問題在文獻中通常被忽略。本論文發現若不考慮這個效應，會低估負群速度與高估增益係數。本論文也一併研究由於光場與鉺離子的交互作用所產生的高階色散對快速光的作用。

關鍵詞：摻鉺光纖放大器，色散，快速光。

Abstract

The project proposal derived the coupled equations of forward and backward spectral field components to describe the nonlinear interaction between the forward and backward waves in optical amplifiers and wavelength converters, e.g. four-wave mixing, Raman effect, and Brillouin effect. The proposed method is able to completely describe the forward and backward waves both in spectral and temporal domains beyond the slowly varying envelope approximation at the expense of time-consuming numerical simulation. Therefore, the use of PC cluster for parallel computing is necessarily for reducing computing time to tolerable level. However, the equipment budget of this project is pruned almost all. As it is hard for simulation, this project studies the optical amplifiers based on power coupled equations instead so that simulation time is tolerable but the original project objective is changed. Nevertheless, this project has published two papers in Optics Express and Optics Communications and submitted a paper to Journal of Optical Society of America B. This report only gives the technical content of the submitted paper but not yet published paper.

A perturbation method is used to study the interaction among signal, pump, and metastable population density for the fast light in an erbium-doped fiber amplifier. The

impact of temporal pump depletion (TPD) on the fast light is investigated, in which TPD is the response of pump power to the temporal variation of metastable population density. The effect of TPD was neglected in the conventional perturbation method shown in literatures because of small signal power assumption. It is found that negative group velocity is under estimated and gain coefficient is over estimated without considering the TPD. The effects of high order dispersions, which are induced by the interaction of the optical fields and erbium ions, on the fast light are also shown.

Keywords: Erbium-doped fiber amplifiers, Dispersion, Fast light

二、緣由與目的

The propagation of the optical pulse in the highly dispersive medium with slow or fast light was interested [1-10]. Several experimental techniques were developed to show such interesting phenomena. It was reported that the slow and fast light can be easily observed by using the effect of coherent population oscillation (CPO) in an erbium-doped fiber amplifier (EDFA) [9,10]. Through the interaction between the fields and erbium ions in an erbium-doped fiber (EDF), there is the spectral absorption dip of narrow bandwidth when pump power is not enough to provide gain. On the contrary, when pump power is high enough, there is the spectral gain dip of narrow bandwidth. According to Kramers-Kronig relations, the EDF becomes a highly dispersive medium for the pulse in the presence of either spectral absorption or gain dip. The spectral absorption and gain dips result in slow and fast light, respectively. Reference [10] showed the case with 9-m EDF strongly pumped by a 980-nm semiconductor laser diode. The 1550-nm input pulse of 0.5 ms width and 0.5 mW power superimposing on a strong continuous wave (CW) control beam of the same wavelength was launched into the pumped EDF. Pulse back-propagation owing to fast group velocity was reported to be experimentally observed and the group index is estimated to be about -4,000.

Because the interested pulse width is much longer than polarization de-phasing time, the interaction of the pulse and the population of doped erbium ions in an EDF can be described by the coupled equations of wave equation and rate equation. Reference [9] used a perturbation method to derive the time delay and gain (loss) coefficient of a sinusoidal modulated wave. This method linearizes the coupled equations by assuming that the power of the sinusoidal modulated wave is much less than that of control beam. Under this assumption, the temporal variation of ground level population density corresponding to the sinusoidal modulated wave can also be assumed to be much less than the steady state population density of ground level corresponding to the control beam. From the linearized coupled equations, the group velocity and gain coefficient of the sinusoidal modulated wave can be obtained. However, in this paper, we show that this perturbation method is not accurate in an EDFA even for the case that the assumption of perturbation is valid. The results numerically solved from the complete coupled equations without linearlization show that the gain coefficient and the absolute value of group velocity are over estimated and under estimated, respectively.

We find that the inaccuracy is due to the temporal pump depletion (TPD) that is not included in the above perturbation method. The pump power depleted by the control beam is not time varying. Pulse depletes metastable population density. Pump power is absorbed more when metastable population density is depleted. The TPD is the pump power temporal variation responding to the temporal variation of the metastable population density absorbed by an optical pulse. In this paper, we develop the perturbation method including the TPD effect. It is shown that our method is accurate compared with the results directly solved from the complete coupled equations. The impact of the TPD on gain coefficient and

group velocity is shown. In addition, the pulse delay time and pulse shape distortion resulting from high order dispersions induced by CPO in an EDFA are also studied.

三、結果與討論

The energy levels of an EDFA can be approximated as a three-level system. However the decay rate from upper level to metastable level is much faster than the decay rate from metastable level to ground level. Because the population density of upper level is negligible, the signal and pump powers in an EDFA can be described by the following equations [11]

$$\frac{\partial P_s}{\partial z}+\frac{n_{gs}}{c}\frac{\partial P_s}{\partial t}= -\left(\alpha_s+\alpha_{ls}\right)P_s+\left(\alpha_{gs}+\alpha_{ls}\right)N_2P_s, \quad (1)$$

$$\frac{\partial P_p}{\partial z}+\frac{n_{gp}}{c}\frac{\partial P_p}{\partial t}= -\left(\alpha_p+\alpha_{lp}\right)P_p+\left(\alpha_{gp}+\alpha_{lp}\right)N_2P_p, \quad (2)$$

where P_s is the signal power including pulse power and control beam power; P_p is forward pump power; n_{gs} and n_{gp} are the group indexes of signal and pump in the absence of doped erbium ions, respectively; c is the light velocity in vacuum; α_s and α_p are the intrinsic fiber loss coefficients at signal and pump wavelengths, respectively; α_{ls} and α_{lp} are the absorption coefficients at signal and pump wavelengths, respectively, which are due to doped erbium ions when population is completely in ground level; α_{gs} and α_{gp} are the gain coefficients at signal and pump wavelengths, respectively, which are due to doped erbium ions when population is completely in metastable level. In Eqs.(1) and (2), $N_2 = n_2 / n_t$ is the normalized metastable population density, in which n_2 and n_t are the population density of the metastable level and doping density, respectively.

The normalized metastable population density can be described by the rate equation [11]

$$\frac{dN_2}{dt}=\frac{1}{\tau}\left(\frac{P_s}{P_s^{th}}+\frac{P_p}{P_p^{th}}\right) -\frac{1}{\tau}\left(1+\frac{P_s}{P_s^{is}}+\frac{P_p}{P_p^{is}}\right)N_2, \quad (3)$$

where τ is the life time of metastable level and

$$P_k^{th}=\frac{A_e h\nu_k n_t}{\alpha_{lk}\tau}, \quad (4a)$$

$$P_k^{is}=\frac{A_e h\nu_k n_t}{(\alpha_{gk}+\alpha_{lk})\tau}, \quad (4b)$$

where k= s and p; $h\nu_s$ and $h\nu_p$ are the photon energies of signal and pump, respectively; and A_e is the effective doping area.

Equations (1)-(3) are the coupled equations that describe the interaction of the optical fields and doped erbium ions. The coupled equations can be numerically solved with the initial conditions

$$P_s(z=0,t)=P_{c0}+P_{a0}(t), \quad (5)$$

$$P_p(z=0,t)=P_{p0}, \quad (6)$$

where P_{c0} is the input control beam power; $P_{a0}(t)$ is the input pulse power envelope; and P_{p0} is the input forward pump power. In this paper, we will consider the Gaussian input pulse

$$P_{a0}(t)=P_{s0}\exp\left[-\left(t/T_0\right)^2\right], \quad (7)$$

where P_{s0} is the pulse peak power and the FWHM pulse width $T_w = 2[\ln(2)]^{1/2}T_0$.

For the considered EDF, τ = 10.5 ms, A_e= 3.14 μm^2, and the EDF length L= 10 m. The delay time contributed from the group index n_g in an EDFA is Ln_g / c = 50 ns for n_g = 1.5. As the delay time is much less than the interested millisecond pulse width, the terms with n_{gs} and n_{gp} in Eqs.(1) and (2), respectively, are negligible. The other numerical parameters of the EDF are: at 980 nm wavelength, α_p = 1.7 dB/km, α_{lp} = 1.04 m^{-1}, and α_{gp} =0; at 1550 nm wavelength, α_s = 0.4 dB/km, α_{ls} = 0.716 m^{-1}, and α_{gs} =

0.845 m^{-1}. We take pulse width T_w= 0.5 ms and pump power P_{p0}= 180 mW to show numerical results in section 4, where the control beam power P_{c0} and peak power P_{s0} are varied.

For CPO effect, it requires pulse power $P_a(z,t)$ be much less than control beam power $P_c(z)$ [12]. Under this requirement, we may take the assumption of small pulse power for linearizing Eqs.(1)-(3), i.e., the power $P_s(z,t) = P_c(z) + P_a(z,t)$, in which $P_c(z) >> |P_a(z,t)|$. For simplicity the z dependence of all variables will not be shown in the following, unless they are specified. The normalized metastable population density can be written as $N_2(t) = N_c + N_a(t)$, where N_c and $N_a(t)$ are the normalized metastable population densities corresponding to P_c and $P_a(t)$, respectively, hence $|N_c| >> |N_a(t)|$. Signal power depletes pump power through metastable population density. The corresponding pump power can be written as $P_p(t) = P_{pc} + P_{pa}(t)$, where P_{pc} and $P_{pa}(t)$ are pump powers corresponding to N_c and $N_a(t)$, respectively, hence $P_{pc} >> |P_{pa}(t)|$.

The powers and normalized metastable population density can be written as

$$P_s(t) = P_c + \int \tilde{P}_a(\Omega)\exp(-i\Omega t)d\Omega, \quad (8)$$

$$P_p(t) = P_{pc} + \int \tilde{P}_{pa}(\Omega)\exp(-i\Omega t)d\Omega, \quad (9)$$

$$N_2(t) = N_c + \int \tilde{N}_a(\Omega)\exp(-i\Omega t)d\Omega, \quad (10)$$

where $\tilde{P}_a(\Omega)$, $\tilde{P}_{pa}(\Omega)$, and $\tilde{N}_a(\Omega)$ are the Fourier transforms of $P_a(t)$, $P_{pa}(t)$, and $N_a(t)$, respectively.

Substituting Eqs.(8)-(10) into Eq.(3) and equating the terms of the same order of magnitude, we have

$$N_c = \left(\frac{P_c}{P_s^{th}} + \frac{P_{pc}}{P_p^{th}}\right)(\omega_c\tau)^{-1}, \quad (11)$$

$$\tilde{N}_a(\Omega) = (\omega_c\tau - i\Omega\tau)^{-1}, \times\left[\left(\frac{\tilde{P}_a}{P_s^{th}} + \frac{\tilde{P}_{pa}}{P_p^{th}}\right) - \left(\frac{\tilde{P}_a}{P_s^{is}} + \frac{\tilde{P}_{pa}}{P_p^{is}}\right)N_c\right] \quad (12)$$

where ω_c is the resonant angular frequency defined according to [9] and

$$\omega_c = \left(1 + \frac{P_c}{P_s^{is}} + \frac{P_{pc}}{P_p^{is}}\right)\tau^{-1}. \quad (13)$$

Substituting Eqs.(8)-(12) into Eqs.(1) and (2), and equating the terms of the same order of magnitude, we have the coupled equations

$$\frac{dP_c}{dz} = -(\alpha_s + \alpha_{ls})P_c + (\alpha_{gs} + \alpha_{ls})N_c P_c, \quad (14)$$

$$\frac{dP_{pc}}{dz} = -(\alpha_p + \alpha_{lp})P_{pc} + (\alpha_{gp} + \alpha_{lp})N_c P_{pc}, \quad (15)$$

$$\frac{d\tilde{P}_a(\Omega)}{dz} = c_{ss}\tilde{P}_a(\Omega) + c_{sp}\tilde{P}_{pa}(\Omega), \quad (16)$$

$$\frac{d\tilde{P}_{pa}(\Omega)}{dz} = c_{pp}\tilde{P}_{pa}(\Omega) + c_{ps}\tilde{P}_a(\Omega), \quad (17)$$

where the coefficients

$$c_{ss} = i\frac{n_{gs}}{c}\Omega - (\alpha_s + \alpha_{ls}) + (\alpha_{gs} + \alpha_{ls}), \times\left[N_c + \left(\frac{P_c}{P_s^{th}} - \frac{P_c}{P_s^{is}}N_c\right)(\omega_c\tau - i\Omega\tau)^{-1}\right], \quad (18)$$

$$c_{sp} = (\alpha_{gs} + \alpha_{ls}) \times\left(\frac{P_c}{P_p^{th}} - \frac{P_c}{P_p^{is}}N_c\right)(\omega_c\tau - i\Omega\tau)^{-1}, \quad (19)$$

$$c_{pp} = i\frac{n_{gp}}{c}\Omega - (\alpha_p + \alpha_{lp}) + (\alpha_{gp} + \alpha_{lp}) \times\left[N_c + \left(\frac{P_{pc}}{P_p^{th}} - \frac{P_{pc}}{P_p^{is}}N_c\right)(\omega_c\tau - i\Omega\tau)^{-1}\right], \quad (20)$$

$$c_{ps} = (\alpha_{gp} + \alpha_{lp}) \times\left(\frac{P_{pc}}{P_s^{th}} - \frac{P_{pc}}{P_s^{is}}N_c\right)(\omega_c\tau - i\Omega\tau)^{-1}. \quad (21)$$

For the case without TPD, the gain coefficient and propagation constant of $\tilde{P}_a(\Omega)$ are the real and imaginary parts of c_{ss}, respectively. The terminology "propagation constant" usually refers to electric field. But for the present analysis, it refers to power envelope. The group index of $P_a(t)$ can be obtained from the derivative of the

propagation constant with respect to Ω at Ω=0. However, TPD always exists. Thus, gain coefficient and propagation constant of $\tilde{P}_a(\Omega)$ must be solved from the coupled equations Eqs.(14)-(17). The following shows the numerical solving procedures.

Step 1:
The CW powers P_c and P_{pc} along the EDF are solved from Eqs.(14) and (15) with the boundary conditions $P_c(z=0)= P_{c0}$ and $P_{pc}(z=0)= P_{p0}$, in which N_c is given by Eq.(11). Note that Eqs.(14) and (15) are independent of Eqs.(16) and (17).

Step 2:
$\tilde{P}_a(z,\Omega)$ and $\tilde{P}_{pa}(z,\Omega)$ are solved from Eqs.(16) and (17) with the boundary conditions $\tilde{P}_a(z=0,\Omega)=1$ and $\tilde{P}_{pa}(z=0,\Omega)=0$. Note that the coefficients given by Eqs.(18)-(21) along the EDF require the CW powers P_c and P_{pc} solved in Step 1.

Step 3:
The transmittance of pulse envelope spectral component of angular frequency Ω at z is $T(z,\Omega)=\tilde{P}_a(z,\Omega)$, which can be written as $T(z,\Omega)=|T(z,\Omega)|\exp[i\theta(z,\Omega)]$ and $\theta(z,\Omega)$ is the phase of $T(z,\Omega)$. The gain coefficient $g_a(z,\Omega)$ and propagation constant $\beta_a(z,\Omega)$ of the spectral component of pulse envelope are

$$g_a(z,\Omega)= \frac{\ln(|T(z+\Delta z,\Omega)|)-\ln(|T(z,\Omega)|)}{\Delta z}, \quad (22)$$

$$\beta_a(z,\Omega)=\frac{\theta(z+\Delta z,\Omega)-\theta(z,\Omega)}{\Delta z}. \quad (23)$$

At the output of the EDFA, the accumulated gain $\gamma_a(\Omega)$ and phase shift $\phi_a(\Omega)$ are

$$\gamma_a(\Omega)=\ln(|T(z=L,\Omega)|), \quad (24)$$

$$\phi_a(\Omega)=\theta(z=L,\Omega). \quad (25)$$

The group delay time along the EDF evaluated at Ω=0 can be calculated as

$$T_{d0}(z)= \int_0^z \frac{\beta_a(z',\Delta\Omega)-\beta_a(z',-\Delta\Omega)}{2\Delta\Omega}dz'. \quad (26)$$

However, we will show in the next section that actual pulse delay time is significantly influenced by high order dispersions. The approximate solution of output pulse shape is

$$P_a(z=L,t)= \int \tilde{P}_{a0}(\Omega)\exp[\gamma_a(\Omega)+i\phi_a(\Omega)-i\Omega t]d\Omega, \quad (27)$$

where $\tilde{P}_{a0}(\Omega)$ is the Fourier transform of input pulse envelope $P_{a0}(t)$. Because the boundary condition $\tilde{P}_a(z=0,\Omega)$ is set to be unit, the approximate solution of temporal pump power variation is

$$P_{pa}(z=L,t)= \int \tilde{P}_{a0}(\Omega)T_{pa}(\Omega)\exp(-i\Omega t)d\Omega, \quad (28)$$

where $T_{pa}(\Omega)=\tilde{P}_{pa}(z=L,\Omega)$ is the spectrum solved in Step 2. The integration in Eqs.(27) and (28) can be numerically calculated with an inverse fast Fourier transform (FFT) routine.

Gain coefficient and propagation constant are even and odd functions, respectively, for the CPO in a two-level system [12]. In the next section, it is shown that the accumulated gain $\gamma_a(\Omega)$ and phase shift $\phi_a(\Omega)$ defined in Eq.(24) and (25) are also even and odd functions, respectively. Thus we may expand them as

$$\gamma_a(\Omega)+i\phi_a(\Omega)= \sum_{\substack{k=0\\ k:even}}^{Q}\frac{1}{k!}\gamma_{ak}\Omega^k + i\sum_{\substack{k=1\\ k:odd}}^{Q}\frac{1}{k!}\phi_{ak}\Omega^k. \quad (29)$$

where Q is an integer; γ_{ak} and ϕ_{ak} are the coefficients obtained by numerically fitting $\gamma_a(\Omega)$ and $\phi_a(\Omega)$ with Eq.(29). For the cases considered in this paper, we take Q= 11. γ_{ak} and ϕ_{ak} represent dispersion coefficients that are the derivatives of $\gamma_a(\Omega)$ and $\phi_a(\Omega)$ at Ω =0, respectively. From Eq.(26), $\phi_{a1}=T_{d0}(z=L)$. In Eq.(29), the even order and odd order terms can be

called the gain dispersion and phase shift dispersion, respectively. For studying the effect of dispersion induced by CPO on pulse shape, we define the partial accumulated gain and phase shift as

$$\gamma_a^{(M)}(\Omega) + i\phi_a^{(M)}(\Omega) = \sum_{\substack{k=0 \\ k:even}}^{M} \frac{1}{k!}\gamma_{ak}\Omega^k + i\sum_{\substack{k=1 \\ k:odd}}^{M} \frac{1}{k!}\phi_{ak}\Omega^k , \qquad (30)$$

where M is an integer not larger than Q; γ_{ak} and ϕ_{ak} are given by Eq.(29). Replacing $\gamma_a(\Omega) + i\phi_a(\Omega)$ in Eq.(27) by $\gamma_a^{(M)}(\Omega) + i\phi_a^{(M)}(\Omega)$, we have the output pulse shape $P_a^{(M)}(t)$ which results from the partial accumulated gain and phase shift.

For the case without TPD, we may solve Eqs.(14) and (16) with the coefficient c_{sp}=0. From the solutions, the output pulse shape, gain coefficient, and propagation constant can be calculated with similar methods shown above.

It is found that the approximate solutions solved from Eqs.(14)-(17) are nearly the same as the exact solutions solved from Eqs.(1)-(3) when the control beam power P_{c0} is about one hundred times larger than the peak pulse power P_{s0}. In this section, we take the ratio $P_{c0}/P_{s0} = 10$ [10], which will result in slight discrepancy between the approximate solution and the exact solution. The propagation characteristics of the fast light with P_{c0}/P_{s0} = 10 and 100 are similar. The cases with P_{c0} = 0.5 mW, 0.1 mW, and 2.5 mW are considered in the following three sub-sections.

(i) P_{c0}= 0.5 mW

Figs. 1(a)-1(f) show the numerical results with P_{c0}= 0.5 mW. Fig. 1(a) shows the input and output pulse shapes, in which the input pulse shape is enlarged one hundred times so that it can be clearly shown. The approximate solutions with and without TPD are also shown in Fig. 1(a). One can see that, without TPD, pulse gain is over estimated and pulse delay time is under estimated. The discrepancy between the exact solution and the approximate solution with TPD is due to the pulse peak power that is not small enough compared with control beam power. Fig. 1(b) shows the pump power temporal variation and normalized metastable population density at EDF output end, in which the approximate solutions $P_{pa}(t)$ and $N_a(t)$ are also shown. $P_{pa}(t)$ and $N_a(t)$ are calculated from Eqs. (28) and (12), respectively. For the case without TPD, $\tilde{P}_{pa}$ = 0 in Eq.(12). One can clearly see that the depletion of metastable population density is under estimated for the case without considering TPD, which leads to the under estimation of CPO effect. Figs. 1(c) and 1(d) show the gain coefficient and propagation constant spectra, respectively, at several distances. In Figs. 1(c) and 1(d), the approximate solutions with and without TPD are shown. At 2.5 m distance, the gain coefficient spectra for the cases with and without TPD are about the same because TPD is not yet significantly built up, so are the propagation constant spectra. After about 5 m distance, for the case without TPD, the gain coefficient and the negative slope of the propagation constant at Ω =0 are over estimated and under estimated, respectively. Thus the pulse gain and negative group velocity are over and under estimated, respectively. Figs. 2(a) and 2(b) show the accumulated gain and phase shift, respectively, for the approximate solutions with and without TPD. From the results, we study the effect of gain dispersion and phase shift dispersion on pulse propagation in the following.

For the case with TPD shown in Fig. 2(a), the gain dip of narrow bandwidth will result in serious high order dispersions. First order dispersion accelerates fast light without pulse distortion. Higher order dispersion not only distorts pulse shape as is shown in Fig. 1(a), but also delays pulse and slows down fast light. Fig. 1(e) shows the pulse peak power delay time T_{peak}, the group delay time T_{d0} calculated from Eq.(26) with TPD, and the group delay time T_{d0} calculated for the case without TPD. One can see that, $|T_{d0}|$ of the case with TPD is much larger than that of the

case without TPD. In Fig. 1(e), T_{peak} is only about a half of T_{d0} with TPD. Average group index can be calculated as $n_{avg} = cT_d/L$, in which T_d is delay time. n_{avg}= -3443, -6176, and -1093 for $T_d = T_{peak}$, T_{d0} with TPD, and T_{d0} without TPD, respectively. Fig. 1(f) shows the output pulse shapes $P_a^{(M)}(t)$ with partial high order dispersions, in which the cases with M= 0, 1, 2, 3, 5, 9, and 11 are shown. In Fig. 1(f), the approximate solution with TPD calculated from Eq.(27) without dispersion expansion is also shown for comparison. From Fig. 1(f), one can see how the combined effect of high odd order dispersions slows down fast light. The peak power delay time of $P_a^{(1)}(t)$ is ϕ_{a1} which agrees with T_{d0} calculated from Eq.(26). The third order dispersion increases pulse delay time and slows down fast light. Thus the absolute value of peak power delay time is decreased. The fifth order dispersion accelerates fast light but it is not able to recover the slow down resulting from the third order dispersion. The dispersions of order larger than fifth further slightly increase pulse delay time and slow down fast light. Including up to the eleventh order dispersion, $P_a^{(11)}(t)$ is about the same as the pulse shape calculated from Eq.(27). Therefore, the group velocity of fast light cannot be defined as the velocity derived from the slope of propagation constant at Ω=0. From Figs. 1(e) and 1(f), one can see the significant modification of group velocity by high order dispersions.

It is interesting to note that, comparing $P_a^{(2)}(t)$ with $P_a^{(1)}(t)$ shown in Fig. 1(f), one can see that the second order gain dispersion significantly narrows pulse width. It can be easily derived that if there only exists the second order gain dispersion, the output FWHM pulse width of the Gaussian input pulse given by Eq.(7) is

$$T_{w2} = 2\left[\ln(2)\left|T_0^2 - 2\gamma_{a2}\right|\right]^{1/2}. \qquad (31)$$

If $\gamma_{a2} < T_0^2/2$, pulse width is narrowed; otherwise, it is broadened. For the case shown in Fig. 1(f), T_0= 0.3 ms (T_w= 0.5 ms) and γ_{a2} = 0.0417 ms^2, we have T_{w2}= 0.137 ms and the pulse is significantly compressed. The compressed pulse width enhances the un-symmetric pulse shape distortion due to the third order dispersion, in which ϕ_{a3} = 0.0133 ms^3. The dispersions of order higher than three smooth out the oscillating tail of $P_a^{(3)}(t)$. The resulting FWHM pulse width is 0.42 ms. In general pulse width may be broadened or narrowed depending on system parameters, such as pulse width, control beam power, and pump power [13] Under small signal assumption, dispersion coefficients change with control beam power and pump power.

(ii) P_{c0}= 0.1 mW

With lower P_{c0}, pump power depletion by amplified control beam power is less and metastable population density (gain) recovery is better. This effect results in less pulse shape distortion but slowing down fast light induced by CPO. Figs. 3(a)-3(f) show the numerical results the same as Figs. 1(a)-1(f), respectively, except that P_{c0}= 0.1 mW and input pulse shape is enlarged five hundred times in Fig. 3(a). Comparing Fig. 3(a) with Fig. 1(a), one can see that the output pulse shape maintains better and the absolute value of pulse peak power delay time is decreased as expected. Comparing Fig. 3(b) with Fig. 1(b), one can see that the depletions of pump power and metastable population density are larger because of higher pulse gain and output pulse power. From Fig. 3(c), at 2.5 m and 5 m distances, the gain coefficients for the cases with and without TPD are about the same because pulse power is still low and TPD is not yet significantly built up, so are the propagation constant spectra shown in Fig. 3(d). At 7.5 m distance, TPD is high enough so that the difference between the cases with and without TPC becomes apparent. From Fig. 3(e), we have average group indexes n_{avg}= -1794, -2223, and -877 for the pulse peak power delay time T_{peak}, T_{d0} with TPD, and T_{d0} without TPD, respectively.

Figs. 2(a) and 2(b) also show the accumulated gain and phase shift, respectively, for the case with P_{c0}= 0.1 mW. The wide bandwidth of the gain dip for this case decreases high order dispersions so that pulse shape maintains better. For this case, γ_{a2} = 0.0101 ms^2, we have T_{w2}= 0.44 ms from Eq.(31) and pulse compression owing to γ_{a2} is slight. From Fig. 3(f), one can see that, including only up to the fourth order dispersion, $P_a^{(4)}(t)$ is about the same as the pulse shape calculated from Eq.(27). The resulting FWHM pulse width is slightly narrowed and is 0.472 ms. The fast light slowed down due to the third order dispersion is less significant than the case with P_{c0}= 0.5 mW.

(iii) P_{c0}= 2.5 mW

From the results shown above, it seems that we may enhance average negative group index and increases the absolute value of pulse delay time by increasing P_{c0}. However the increase of input control beam power not only enhances the first order dispersion coefficient ϕ_{a1} , but also higher order dispersion coefficients ϕ_{ak} (k>1). The enhanced higher order dispersion coefficients may result in serious pulse shape distortion and slowing down fast light. For example, Figs. 4(a) and 4(b) show the same case as Figs. 1(a) and 1(f), respectively, except that P_{c0}= 2.5 mW and input pulse shape is enlarged twenty times in Fig. 4(a). One can see that ϕ_{a1} = -0.41 ms, which is about 80% pulse width, but the combined effect of higher order dispersions decreases pulse peak power delay time to be -0.144 ms (-4320 average group index) and seriously distorts pulse shape. From Fig. 4(b), $P_a^{(11)}(t)$ is not able to approximate the pulse shape calculated from Eq.(27). The inclusion of more high order terms is required. It is noticed that $P_a^{(2)}(t)$ is slightly broadened instead of narrowing. For this case, γ_{a2} = 0.0918 ms^2, which is large enough to broaden pulse width. From Eq.(31), T_{w2}= 0.509 ms. Because T_{w2} is close to 0.5 ms input pulse width, $P_a^{(2)}(t)$ almost overlaps $P_a^{(1)}(t)$ in Fig. 4(f). Careful system parameter optimization is able to improve the absolute value of peak power delay time under a certain constraint of pulse shape distortion [13]. However, as the first order dispersion is enhanced, higher order dispersions are usually enhanced accordingly. The optimization should compromise between the first order dispersion and higher order dispersions.

四、計畫成果自評

Fast light can be realized by utilizing the CPO effect in an EDFA, in which a pulse superimposing on a strong CW control beam is launched into the EDFA. Pulse depletes metastable population density. Pump power is absorbed more when metastable population density is depleted. In literatures, the perturbation method analyzing the fast light in an EDFA did not consider this pump power depletion. Thus the CPO effect is under estimated and the derived gain coefficient and propagation constant are inaccurate. We have developed the perturbation method for solving the time varying parts of the signal power, pump power, and metastable population density. The coupled equations of the spectral components of the signal power, pump power, and metastable population density are derived. From the coupled equations, we can accurately solve the gain coefficient and propagation constant of the fast light in an EDFA. It is found that pulse gain and negative group velocity are over and under estimated, respectively, if temporal pump depletion is not considered. From the solved gain coefficient and propagation constant, we also study the pulse delay time and shape distortion resulting from high order dispersions induced by CPO. The gain dispersion resulting from accumulated gain is shown. Accumulated gain is the integration of gain coefficient along an EDF, which is an even function of frequency. The second order gain dispersion may symmetrically broaden

or compress pulse depending on the value of its coefficient. The changes of pulse shape by higher even order gain dispersions are complicated because of the combined effect with high odd order phase shift dispersions. The phase shift dispersion results from the accumulated phase shift, which is the integration of propagation constant along an EDF and is an odd function of frequency. The first order phase shift dispersion un-distortedly leads to negative pulse delay time. Higher odd order phase shift dispersions un-symmetrically distort pulse shape and change pulse delay time. For the shown examples, the third order and fifth order dispersions result in slowing down and accelerating fast light, respectively. Thus the group velocity of fast light cannot be simply defined as the velocity derived from the first derivative of propagation constant. The presented perturbation method can also be applied to analyzing the fast light in the other resonant medium with optical pumping.

The technical content shown above has been submitted to Journal of Optical Society of America B [14]. In addition, this project has published two papers regarding the designs of Raman fiber amplifiers in Optics Express and Optics Communications [15,16].

五、參考文獻

[1] R. Y. Chiao, "Superluminal (but casual) propagation of wave packets in transparent media with inverted atomic populations," Phy. Rev. A **48**, R34-R37 (1993).

[2] E. L. Bolda, J. C. Garrison, and R. Y. Chiao, "Optical pulse propagation at negative group velocities due to a nearby gain line," Phy. Rev. A **49**, 2938–2947 (1994).

[3] L. V. Hau, S. E. Haris, Z. Dutton, and C. H. Behroozi, "Light speed reduction to 17 meters per second in an ultracold atomic gas," Nature **397**, 594-598 (1999).

[4] L. J. Wang, A. Kuzmmich, and A. Dogariu, "Gain-assisted superluminal light propagation," Nature **406**, 277–279 (2000).

[5] Md. A. I. Talukder, Y. Amagishi, and M. Tomita, "Superluminal to subluminal transition in the pulse propagation in a resonant absorbing medium," Phy. Rev. Lett. **86**, 3546-3549 (2001).

[6] M. S. Bigelow, N. N. Lepeshkin, and R. W. Boyd, "Observation of ultraslow light propagation in a ruby crystal at room temperature," Phy. Rev. Lett. **90**, 113903 (2003).

[7] M. S. Bigelow, N. N. Lepeshkin, and R. W. Boyd, "Ultra-slow and superluminal light propagation in solids at room temperature," J. Phy.: Cond. Mat. **16**, R1321-R1340 (2004).

[8] G. Dolling, C. Enkrich, M. Wegener, C. M. Soukoulis, and S. Linden, "Simultaneous negative phase and group velocity of light in a metamaterial," Science **312**, 892–894 (2006).

[9] A. Schweinsberg, N. N. Lepeshkin, M. S. Bigelow, R. W. Boyd, and S. Jarabo, "Observation of superluminal and slow light propagation in erbium-doped optical fiber," EuroPhys. Lett. **73**, 218-224 (2006).

[10] G. M. Gehring, A. Schweinsberg, C. Barsi, N. Kostinski, and R. W. Boyd," Observation of backward pulse propagation through a medium with a negative group velocity," Science **312**, 895–897 (2006).

[11] E. Desurvire, *Erbium-Doped Fiber Amplifiers, Principles and Applications*, (John Wiley & Sons, New York, USA, 1994).

[12] R. Boyd, *Nonlinear Optics*, 2nd ed., (Elsevier Science, New York, USA, 2003).

[13] H. Shin, A. Schweinsberg, G. Gehring, K. Schwertz, H. J. Chang, R. W. Boyd, Q-H. Park, and D. J. Gautheir, " Reducing pulse distortion in fast-light pulse propagation through an erbium-doped fiber amplifier," Opt. Lett. **32**, 906–908 (2007).

[14] S. Wen and S. Chi, "Propagation characteristics of the fast light in an

erbium-doped fiber amplifier," submitted to JOSA B.
[15] S. Wen and S. Chi," DCF-based fiber Raman amplifiers with fiber grating reflectors for tailoring accumulated-dispersion spectra," Opt. Comm., **272**, pp. 247-251, 2007.
[16] S. Wen, C.-C. Chen, and J.-W. Ou," Optimizing the incoherent pump spectrum of low-gain-ripple distributed fiber Raman amplifiers for a given main incoherent pump wavelength," Opt. Express., **15**, pp. 45-55, 2007.

六、圖表

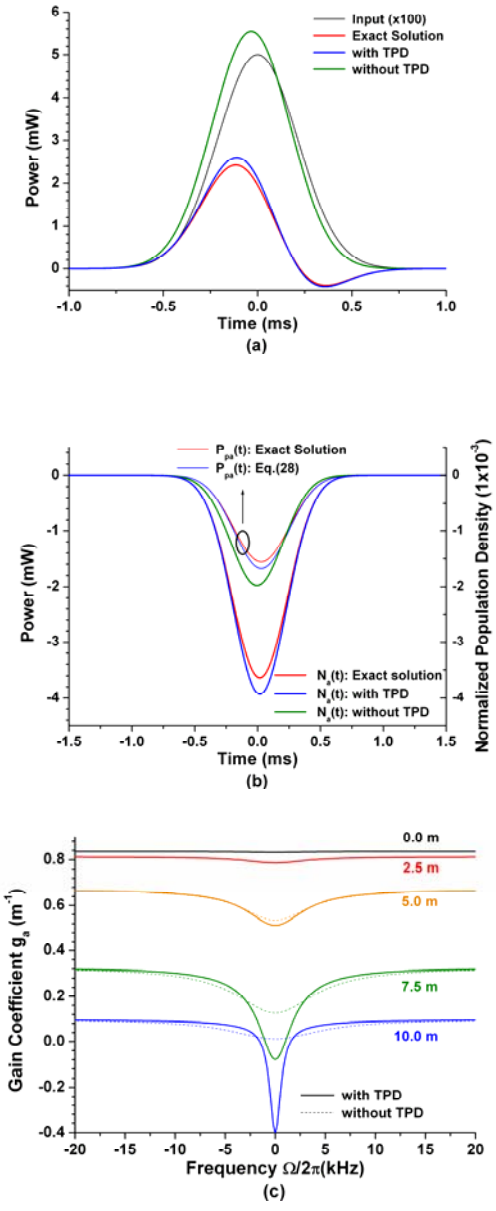

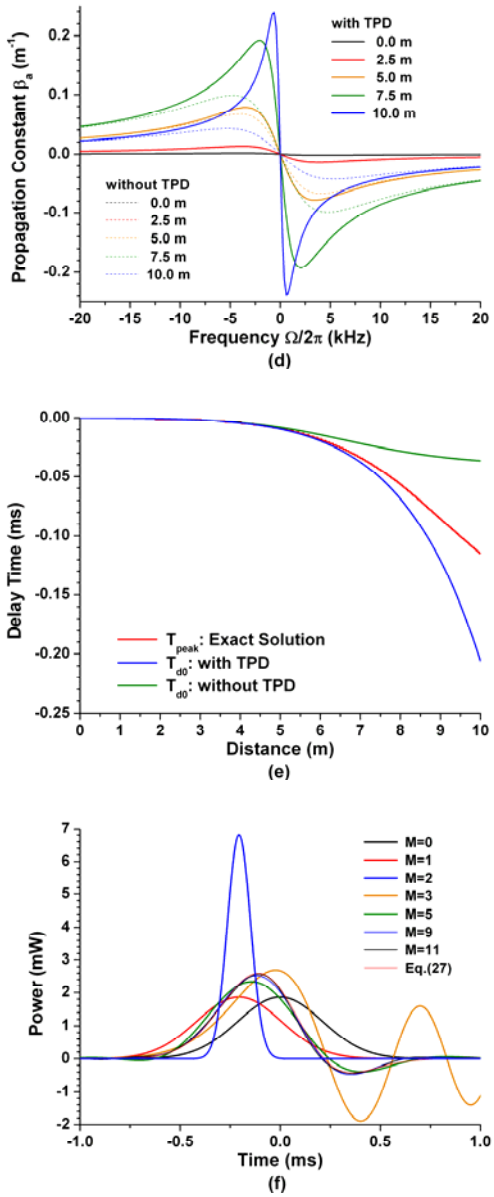

Figure 1: With input control beam power P_{c0}= 0.5 mW, (a) input and output pulse shapes, (b) pump power temporal variation and normalized metastable population density at EDF output end, (c) gain coefficient spectra at several distances, (d) propagation constant spectra at several distances, (e) pulse peak power delay time T_{peak} and the group delay time T_{d0} along EDF evaluated at Ω=0, and (f) output pulse shapes $P_a^{(M)}(t)$ synthesized up to several M dispersion orders and the approximate solution with TPD calculated from Eq.(27) without dispersion expansion. The exact solution is solved from Eqs.(1)-(3). The approximate solutions with and without TPD are shown in figures (a)-(e) for comparison.

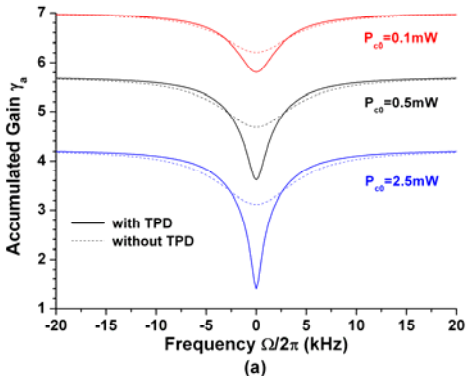

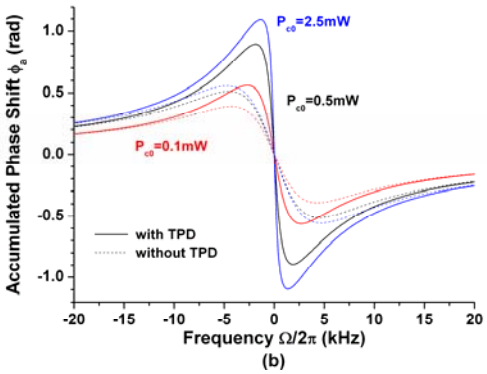

Figure 2: (a) Accumulated gain spectra and (b) accumulated phase shift spectra for the cases with P_{c0}= 0.1 mW, 0.5 mW, and 2.5mW.

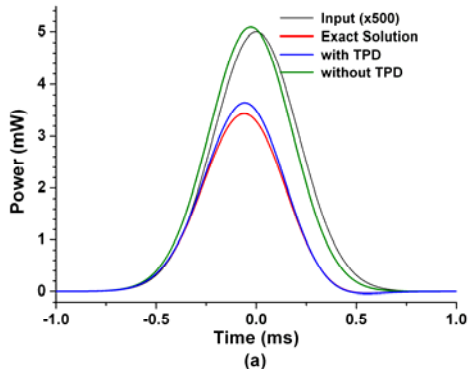

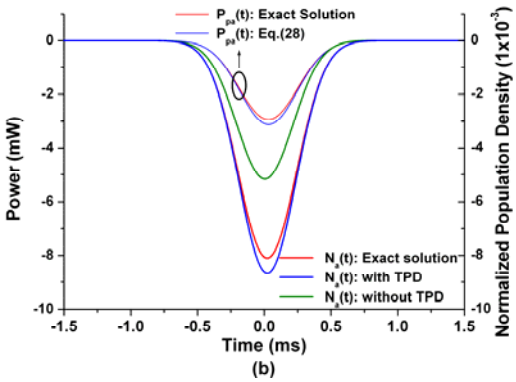

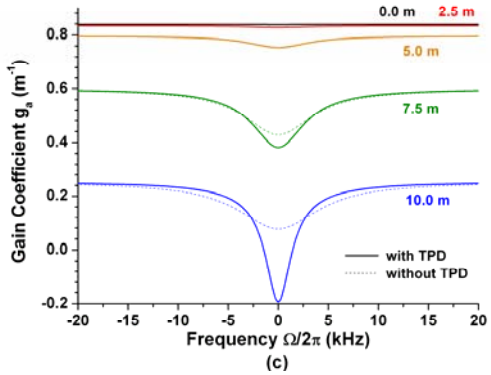

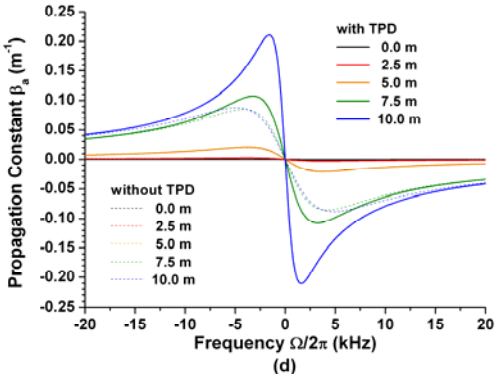

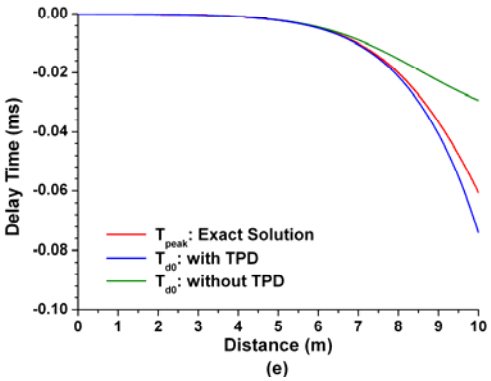

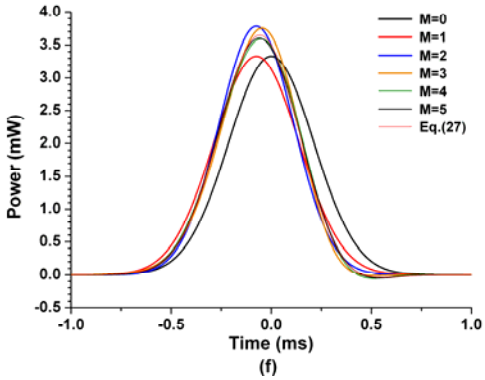

Figure 3: The same as Fig. 1 except that input control beam power P_{c0}= 0.1 mW.

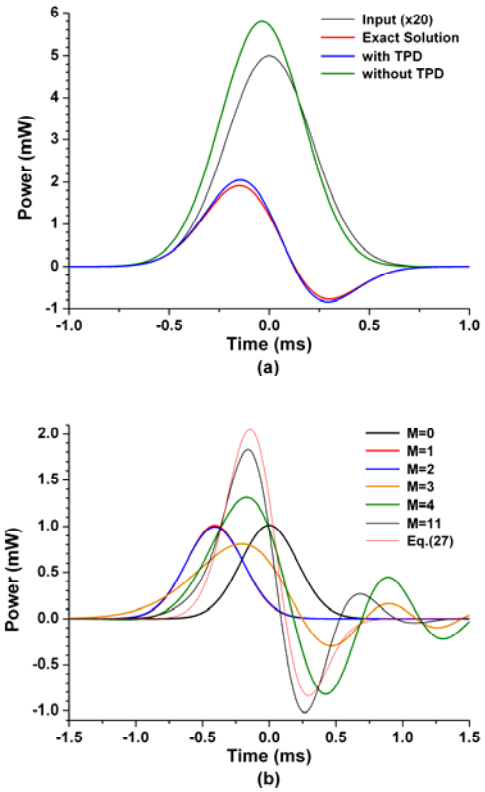

Figure 4: With input control beam power P_{c0}= 2.5 mW, (a) input and output pulse shapes, and (b) output pulse shapes $P_a^{(M)}(t)$ synthesized up to several M dispersion orders and the approximate solution with TPD calculated from Eq.(27) without dispersion expansion. In figure (b), the corresponding values of M are also indicated by arrows. The exact solution is solved from Eqs.(1)-(3). The approximate solutions with and without TPD are shown in figure (a) for comparison.